IOP PUBLISHING NANOTECHNOLOGY
Nanotechnology **18** (2007) 215601 (4pp) doi:10.1088/0957-4484/18/21/215601

Iron nanoparticle formation in a metal–organic matrix: from ripening to gluttony

Christian Klinke[1,2,4] **and Klaus Kern**[2,3]

[1] Institute of Physical Chemistry, University of Hamburg, D-20146 Hamburg, Germany
[2] Institut de Physique des Nanostructures, Ecole Polytechnique Fédérale de Lausanne, CH-1015 Lausanne, Switzerland
[3] Max-Planck-Institute for Solid State Research, D-70569 Stuttgart, Germany

E-mail: klinke@chemie.uni-hamburg.de

Received 6 February 2007, in final form 29 March 2007
Published 27 April 2007
Online at stacks.iop.org/Nano/18/215601

Abstract
A simple method for the fabrication of metal nanoparticles is introduced. Heating metal–organic crystals in vacuum results in the formation of well-defined metal particles embedded in a carbon matrix. The method is demonstrated for iron phthalocyanine. At 500 °C homogeneously distributed iron nanoparticles with a reasonably narrow size distribution form by nucleation and ripening. After this initial phase the formation kinetics changes drastically. The particles move in the matrix to incorporate material. The 'gluttony' phase shows astonishing similarities with the search for nutrition of living micro-organisms. Particle formation, ripening and gluttony are followed *in situ* by transmission electron microscopy.

S Supplementary data are available from stacks.iop.org/Nano/18/215601

Nanometre-sized particles of magnetic metals have been attracting substantial interest in basic and applied research for many years [1–4]. This activity is mainly driven by the envisaged application of such nanoparticles in high-density data storage [5], in magnetic resonance imaging [6, 7], and as catalysts [8, 9]. In many cases they show improved or even new properties due to their size in the nanometre range [10]. State-of-the-art production methods of metal nanoparticles include arc discharge [2], colloidal chemistry [11], sputtering or laser ablation [12], and ripening from gel-like films [8]. Each method has its specific advantages and disadvantages. Critical issues are the stability of the particles with time, their protection against oxidation [13], and the control of their size and shape [14]. Here we present a novel, simple method to produce inherently protected iron nanoparticles. They are generated by heating iron phthalocyanine crystallites in vacuum. The particles exhibit a narrow diameter distribution and ferromagnetic hysteresis. The obtained structures and particles were imaged by scanning electron microscopy (SEM) and transmission electron microscopy (TEM) after the heat treatment. *In situ* TEM observations show that the formation process is a complex mechanism, taking place basically in two phases: a first classical nucleation, growth and ripening phase, and a second phase in which the particles move in the matrix to incorporate material. The second phase shows astonishing similarities with the search for nutrition of living micro-organisms.

Iron phthalocyanine ($C_{32}H_{16}N_8$)Fe (FePc, figure 1(a) (inset)) as purchased is a black powder consisting of bacillary crystallites. It is a macrocyclic compound having an alternating nitrogen–carbon aromatic ring structure coordinating a central iron atom. Figure 1(a) shows such crystals dispersed on a silicon surface out of a dried ethanolic suspension. Such samples were heated in a furnace for 30 min at 500 °C at a base pressure of $<2 \times 10^{-5}$ mbar. During heating the pressure increased due to sublimation of FePc molecules, and evaporation of nitrogen and hydrogen from decomposed FePc molecules. SEM micrographs show that the crystals transform into skeleton-like structures (figure 1(b)). A closer look at the structures reveals a capillary network which probably consists of tubular or flaky carbon (figure 1(b) (inset)). TEM allows

[4] Author to whom any correspondence should be addressed.

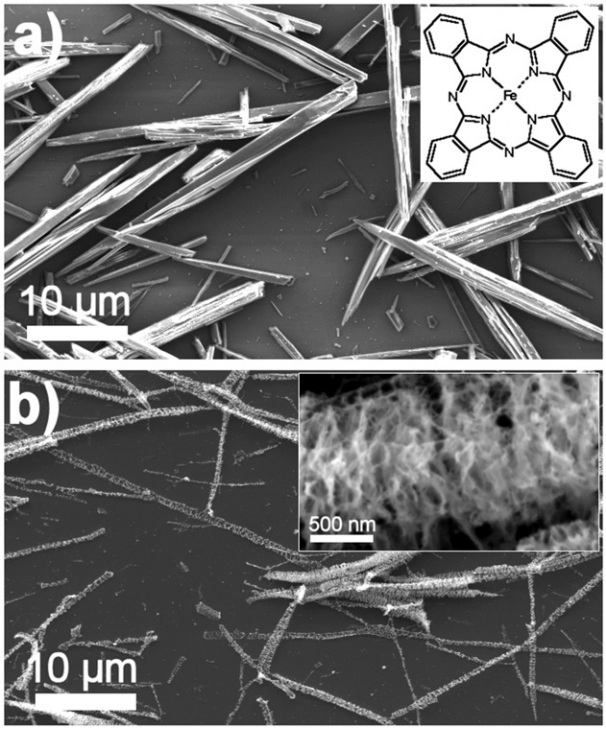

Figure 1. SEM micrographs of (a) as-purchased FePc crystals dispersed on a silicon surface (inset: iron phthalocyanine molecule ($C_{32}H_{16}N_8$)Fe), (b) the obtained skeleton structure after heating for 30 min at 500 °C at a base pressure of $<2 \times 10^{-5}$ mbar (inset: close-up of the transformed crystals).

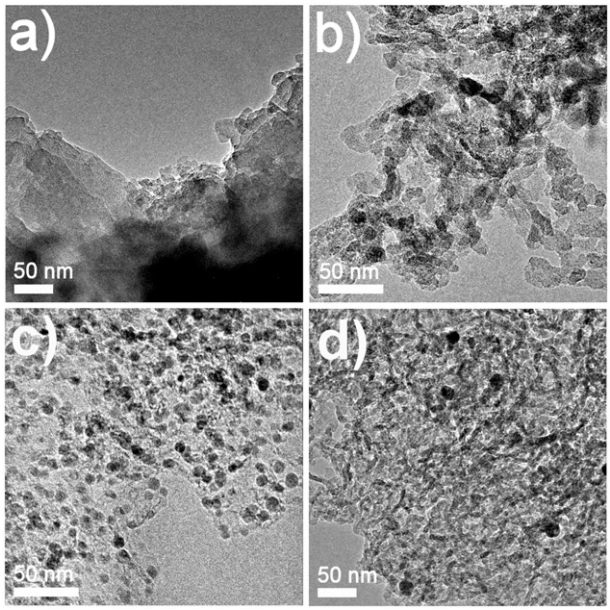

Figure 2. TEM micrographs of a time series of FePc heated at 500 °C in a vacuum furnace for (a) 2 min, (b) 3 min, (c) 10 min, (d) 30 min.

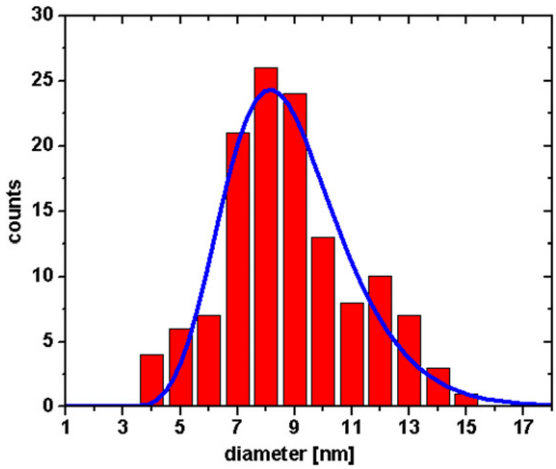

Figure 3. A statistical analysis of 130 particles after a heat treatment of 10 min at 500 °C (figure 2(c)) allows fitting the distribution of particle diameters with a log-normal distribution. The fitting parameters for the log-normal distribution (continuous curve) $y = A \times \exp[-(\ln(x) - \mu)^2/2\sigma^2]/(\sqrt{(2\pi)} \times \sigma \times x)$ are the amplitude $A = 123.4$, the standard deviation $\sigma = 0.24$ and mean $\mu = 2.15$. The function peaks at $\exp(\mu - \sigma^2) = 8.1$ nm with the standard deviation of $\sqrt{(\exp(2\mu + \sigma^2) \times (\exp(\sigma^2) - 1))} = 2.15$ nm. (This figure is in colour only in the electronic version)

the investigation of the internal structure. Heating of FePc crystals on SiO_2-covered TEM grids in a furnace shows that nanoparticles form in the crystals with elapsing time. Figure 2 demonstrates this transformation: after 2 min heating in a furnace at 500 °C almost no change is observed, but after 3 min the TEM images already show cleft structures. After 10 min the nanoparticles become clearly visible and after 30 min they coarsen to bigger clusters. TEM diffraction measurements after the heat treatment show that the nanoclusters consist of fcc-Fe at room temperature. A statistical analysis of 130 particles after a heat treatment of 10 min at 500 °C (figure 2(c)) reveals a reasonably narrow size distribution peaking at 8.1 nm with a standard deviation of 2.15 nm (figure 3).

In situ heating of the samples in a TEM unveils that the transition starts around 400 °C, and all individual crystals transform into iron/carbon structures. In this case, the samples were not observed during the whole process but just sporadically during heating. In other experiments, the samples were heated from ambient temperature up to 700 °C under constant observation. In this case, the transition was directly observed between 600 and 700 °C.[5] In this temperature range the crystals transform in a few minutes. Figure 4 shows a series of video images of the development of an individual crystal. In this case the formation of the metal particles starts at 622 °C, then at 662 °C they are getting bigger, and at 701 °C they begin to move in the matrix, absorbing material on their way. The nanoparticles move randomly in the Fe/C structure of the original FePc crystal, leaving empty space behind. This migration gives rise to the characteristic final structure (see also the video streams in the Supporting Information available at stacks.iop.org/Nano/18/215601). The particle movement corresponds to a *self-avoiding random walk* and can be simulated by a simple algorithm: in the simulations the FePc crystals are represented by a two-dimensional (2D) matrix. The matrix positions are 'filled' with pseudo particles with a size of

[5] The difference in transition temperature might be due to a decomposition of organic molecules of the residual pressure by the electron beam and a deposition of amorphous carbon on the samples which inhibits an immediate transformation of the FePc crystals.

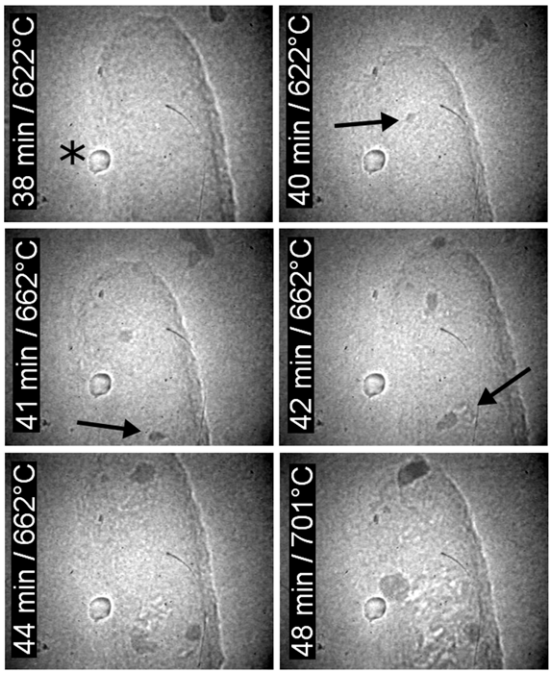

Figure 4. TEM micrographs of an individual FePc crystal heated *in situ* up to a temperature of 701 °C. The size of this video image is about 100 × 80 nm^2. First, the particles (arrows) grow by a ripening process. Later they start to acquire material by moving in the matrix (* impurity of the CCD camera).

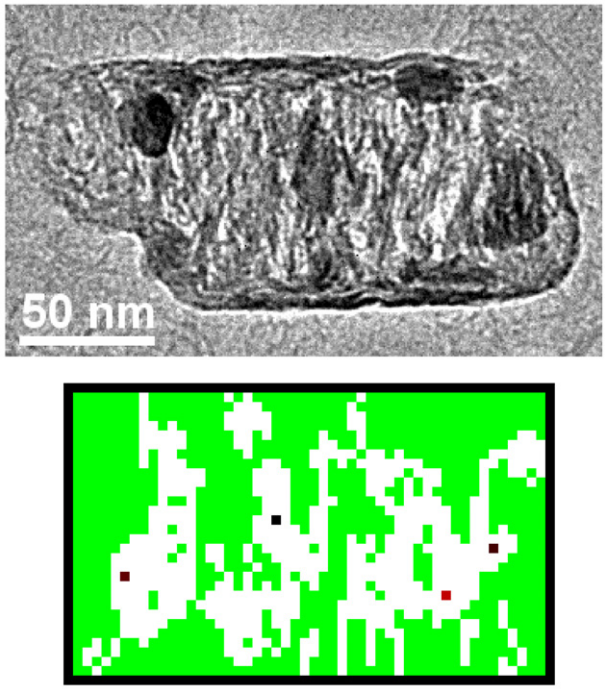

Figure 5. Comparison of an *in situ* transformed FePc crystallite and a simulated self-avoiding random walk of pseudo particles with a size of about 3 nm (green: pristine material; red-black: pseudo particles with increasing amount of absorbed material).

about 3 nm, the 'nutrition' units. Then, a random distribution of germs is spread in the matrix. The migration algorithm assumes that each germ picks up a random neighbour unit and moves to its location, leaving behind a void location where it has been before. In principle, each location is equal as long as there is 'food'; empty locations are disregarded. Additionally to the random walk we implemented a slight anisotropy in a way that the absorption in vertical direction is favoured in order to mimic the crystal structure of FePc. Proceeding with this algorithm for each germ leads to a final structure similar to the transformed FePc crystals. The germs stop their movement when there is no direct neighbouring nutrition unit left. Figure 5 shows a comparison of an *in situ* transformed FePc crystallite and a simulated transformation.

The remarkable behaviour of the FePc crystallites under heating can be explained basically with two distinguished growth phases. First, annealing in the temperature regime between 400 and 500 °C leads to a breaking of intramolecular bonds. Hydrogen and nitrogen recombine and evaporate as H_2 and N_2. In this initial phase iron is quite mobile and can diffuse since it is atomically distributed in the remaining carbon matrix and weakly bound. Nanoparticles are generated by stationary germs which grow by attracting material from the environment [8] and eventually ripen. In a second phase, at an increased temperature of about 650 °C, the nanoparticles start to move in the carbon matrix, absorbing more material. This behaviour results in a separation of iron and carbon. The carbon is reorganized by the moving iron clusters and forms the characteristic final web-like structure. This effect is similar to the movement of biological cells, known as phagokinetic tracks [15–17] and tracks of surface alloy islands [18]. Diffusion, ripening, and surface (energy) minimization enables the iron to form bigger roundish aggregates. Additionally, the surface energy can be lowered when the iron aggregates are surrounded by carbon. This leads to a 'hiding' of particles in the pockets. The particles must avoid free surface facets (capillary forces). In turn, this leads to a growth of the particles into the material, out of the holes into the self-created cavities. Since the particles, by undergoing this process, always stay in contact with non-transformed material, they can absorb more and more iron (from the stock). The movement stops and leaves the final characteristic structure behind when there is no more iron left in the direct proximity. In the long run, particles can diffuse over large distances and form extended aggregates. As larger particles move more slowly, a relatively narrow size distribution can be obtained at intermediate stages. Further optimization of the process parameters might lead to an even sharper size distribution.

The iron/carbon powder obtained after heating of macroscopic amounts of FePc for 10 min at 500 °C shows ferromagnetic hysteresis. SQUID measurements reveal that both the coercive field and the remanent magnetization increase as the temperature decreases. Furthermore, the iron/carbon structures are active catalysts for the chemical vapour deposition (CVD) growth of carbon nanotubes. In an experiment using a tube furnace at 650 °C, multi-wall nanotubes grow nicely using acetylene as carbon source. They are of similar quality as the CVD tubes obtained using iron-containing solutions as catalyst [19]. As other groups have shown, carbon nanotubes can also be produced directly by pyrolysis of iron phthalocyanine [20–22].

To conclude, under heating in vacuum FePc crystallites decompose into iron nanoparticles embedded in a carbon matrix. By means of *in situ* TEM investigations we observed the remarkable formation mechanism of these structures. A classical nucleation, growth and ripening phase is succeeded at higher temperature by a gluttony phase, during which the particles move in the carbon matrix, acquiring further material. The synthesis method is very appealing due to its simplicity. It involves only one precursor and only one heating step. The method was demonstrated for the fabrication of iron nanoparticles but can easily be generalized to other systems since there are over 70 ions known which can be accommodated by phthalocyanine [23].

Experimental methods

Iron phthalocyanine (FePc) was suspended in ethanol, sonicated for 5 min, and dried on silicon oxide surfaces. The samples were then submitted to a tubular vacuum furnace at 500 °C and $<2\times10^{-5}$ mbar for different time periods by means of a transfer rod.

SEM characterizations were performed to analyse the structures in plan view. A Philips XL 30 microscope equipped with a field-emission gun operating at an acceleration voltage between 3 and 5 kV, a working distance of typically 10 mm, and in secondary electron image mode, was used.

The internal structure of the samples was controlled by TEM. For this purpose a Philips EM 430 microscope equipped with a Gatan image plate operating at 300 kV was used. The FePc crystallites were dispensed on TEM grids covered with a thin SiO_2 film. The transformation of FePc crystals as a function of temperature to a carbon matrix with embedded iron particles was directly observed and video-taped *in situ* in a TEM equipped with a resistively heatable sample holder.

The magnetic properties of the obtained Fe/C powder were measured with a quantum design SQUID magnetometer (MPMS7). This apparatus, which has a sensitivity of $<10^{-6}$ emu (corresponding to 1 μg of powder), is equipped with a cryogenic sample stage which permits control of the temperature between 1.8 and 340 K. The applied field varied between ±45 kOe.

Acknowledgments

The Swiss National Science Foundation (SNF) is acknowledged for financial support. The electron microscopy was performed at the Centre Interdépartmental de Microscopie Electronique (CIME) of EPFL.

References

[1] Wegrowe J E, Fruchart O, Nozieres J P, Givord D, Rousseaux F, Decanini D and Ansermet J Ph 1999 Arrays of ultrathin monocrystalline submicrometer-sized Fe dots: Neel–Brown relaxation and activation volume *J. Appl. Phys.* **86** 1028

[2] Bonard J M, Seraphin S, Wegrowe J E, Jiao J and Chatelain A 2001 Varing the size and magnetic properties of carbon-encapsulated cobalt particles *Chem. Phys. Lett.* **343** 251

[3] Brunsman E M *et al* 1994 Magnetic properties of carbon-coated, ferromagnetic nanoparticles produced by a carbon-arc method *J. Appl. Phys.* **75** 5882

[4] Zeng H, Li J, Liu J P, Wang Z L and Sun S 2002 Exchange-coupled nanocomposite magnets by nanoparticle self-assembly *Nature* **420** 395

[5] Warne B, Kasyutich O I, Mayes E L, Wiggins J A L and Wong K K W 2000 Self assembled nanoparticulate Co:Pt for data storage applications *IEEE Trans. Magn.* **36** 3009

[6] Cunningham C H, Arai T, Yang P C, McConnell M V, Pauly J M and Conolly S M 2005 Positive contrast magnetic resonance imaging of cells labeled with magnetic nanoparticles *Magn. Reson. Med.* **53** 999

[7] Pankhurst Q A, Connolly J, Jones S K and Dobson J 2003 Applications of magnetic nanoparticles in biomedicine *J. Phys. D: Appl. Phys.* **36** R167

[8] Klinke C, Bonard J M and Kern K 2004 Formation of metallic nanocrystals from gel-like precursor films for CVD nanotube growth: an *in situ* TEM characterization *J. Phys. Chem.* B **108** 11357

[9] Hernadi K, Couteau E, Umek P, Miko C, Seo J W, Forro L, Croci M, Klinke C, Chauvin P and Bonard J M 2002 Controlled growth and applications of carbon nanotubes *Chimia* **56** 547

[10] Batlle X and Labarta A 2002 Finite-size effects in fine particles: magnetic and transport properties *J. Phys. D: Appl. Phys.* **35** R15

[11] Shevchenko E V, Talapin D V, Schnablegger H, Kornowski A, Festin O, Svedlindh P, Haase M and Weller H 2003 Study of nucleation and growth in the organometallic synthesis of magnetic alloy nanocrystals: the role of nucleation rate in size control of CoPt3 nanocrystals *J. Am. Chem. Soc.* **125** 9090

[12] Ayyub P, Chandra R, Taneja P, Sharma A K and Pinto R 2001 Synthesis of nanocrystalline material by sputtering and laser ablation at low temperatures *Appl. Phys.* A **73** 67

[13] Zeng H, Zheng M, Skomski R, Sellmyer D J, Liu Y, Menon L and Bandyopadhyay S 2000 Magnetic properties of self-assembled Co nanowires of varying length and diameter *J. Appl. Phys.* **87** 4718

[14] Cowburn R P, Koltsov D K, Adeyeye A O and Welland M E 2000 Lateral interface anisotropy in nanomagnets *J. Appl. Phys.* **87** 7067

[15] Albrecht-Buehler G 1977 Phagokinetic tracks of 3T3 cells: parallels between the orientation of track segments and of cellular structures which contain actin or tubulin *Cell* **12** 333

[16] Ikeda W, Kakunaga S, Takekuni K, Shingai T, Satoh K, Morimoto K, Takeuchi M, Imai T and Takai Y 2004 Nectin-like molecule-5/Tage4 enhances cell migration in an integrin-dependent, nectin-3-independent manner *J. Biol. Chem.* **279** 18015

[17] Parak W J, Boudreau R, Le Gros M, Gerion D, Zanchet D, Micheel C M, Williams S C, Alivisatos A P and Larabell C 2002 Cell motility and metastatic potential studies based on quantum dot imaging of phagokinetic tracks *Adv. Mater.* **14** 882

[18] Schmid A K, Bartelt N C and Hwang R Q 2000 Alloying at surfaces by the migration of reactive two-dimensional islands *Science* **290** 1561

[19] Klinke C, Bonard J M and Kern K 2001 Comparative study of the catalytic growth of patterned carbon nanotube films *Surf. Sci.* **492** 195

[20] Huang S, Dai L and Mau A W H 1999 Nanotube 'crop circles' *J. Mater. Chem.* **9** 1221

[21] Huang S and Dai L 2002 Microscopic and macroscopic structures of carbon nanotubes produced by pyrolysis of iron phthalocyanine *J. Nanopart. Res.* **4** 145

[22] Segura R A, Ibanez W, Soto R, Hevia S and Häberle P 2006 Growth morphology and spectroscopy of multiwall carbon nanotubes synthesized by pyrolysis of iron phthalocyanine *J. Nanosci. Nanotechnol.* **6** 1945

[23] McKeown N B, Makhseed S and Budd P M 2002 Phthalocyanine-based nanoporous network polymers *Chem. Commun.* **23** 2780